Systematical behavior of even-A polonium isotopes

W. Younes and J. A. Cizewski
Department of Physics and Astronomy, Rutgers University, New Brunswick, New Jersey 08903
(Received 17 July 1996)

The energy systematics of even-A, neutron-deficient polonium isotopes have been previously observed down to $A=194$. The low-lying states display a gradual approach to the equal spacings of a harmonic vibrator, exceeding this limit for the first time in ^{194}Po. We have successfully modeled these energy systematics using the particle-core model and have applied the quasiparticle random phase approximation to extract microscopic wave functions for the collective 2_1^+ states and predict $B(E2;2_1^+\rightarrow 0_1^+)$ values. We are able to explain the Po trends in terms of the overlaps of the wave functions of valence particles, overlaps which are enhanced when particles occupy the high-j proton $1h_{9/2}$ and neutron $1i_{13/2}$ orbitals. We find little evidence for particle-hole excitations across the $Z=82$ shell gap. [S0556-2813(97)00803-0]

PACS number(s): 21.60.Cs, 21.60.Ev, 21.60.Jz, 27.80.+w

I. INTRODUCTION

The proton-neutron interaction plays a fundamental role in the onset of collectivity in nuclei. This feature of the nuclear residual interaction has long been known [1] and can be understood simply in terms of the overlap of single-particle orbitals [2]. In light nuclei, where protons and neutrons fill the same shell, the Pauli exclusion principle allows many more configurations of pairs of unlike particles (p-n) in equivalent orbitals ($j_1=j_2$) than like (p-p or n-n) particles. The larger number of interaction matrix elements in the p-n configurations leads to greater mixing of the wave functions and, therefore, often produces very collective states. In medium and heavy nuclei, valence protons and neutrons do not occupy the same orbitals. However, as the number of valence particles changes across the shells, both protons and neutrons can occupy high-j orbitals. A simple semiclassical argument can then be used [2] to show that, when $j_p\approx j_n\gg 1$, the angular overlap between coupled pairs of protons and neutrons is large. Furthermore, when the number of nodes $n_p=n_n$ and the orbital angular momenta $\ell_p\approx\ell_n$, the radial overlap between proton and neutron wave functions is maximized as well [1]. Therefore, the proton-neutron interaction should be strongly enhanced when valence particles occupy the $\pi 1g_{7/2}$ and $\nu 1h_{11/2}$ orbitals in the Sn region, or the $\pi 1h_{9/2}$ and $\nu 1i_{13/2}$ orbitals in the Pb region.

This simple mechanism emphasizes the importance of particular proton and neutron orbitals which drive the approach to collective motion. As the middle of the (neutron) shell is approached in many nuclei, the residual p-n interaction is often strong enough to reduce the (proton) shell gap and allow particles to be excited from the shell below, leaving active holes behind. These particle-hole (p-h) excitations can precipitate the onset of collectivity by promoting particles into deformation-driving configurations of overlapping orbitals. These configurations then give rise to collective bands, which can coexist and mix with normally deformed states. The experimental evidence for such structures comes mainly [3] from electric monopole ($E0$) transition strengths, which are enhanced when deformed p-h excitations and normal spherical states are mixed; $B(E2)$ strengths, which follow selection rules for different shapes and provide an indirect measure of deformation; and single-particle occupation probabilities determined from transfer reactions. An extensive study of both theoretical and experimental aspects of this excitation mechanism can be found in [3].

In the cadmium ($Z=48$) and mercury ($Z=80$) nuclei, $4h$-$2p$ proton configurations have been clearly identified at low excitation energies. In contrast, the existence of low-lying $4p$-$2h$ excitations in the tellurium isotopes is not as well established [4,5]. The case against $4p$-$2h$ intruder configurations has also been made elsewhere for ^{196,198}Po [6] and ^{194}Po [7]; these arguments will not be repeated here. Instead we present a complete and consistent theoretical description of the low-lying structure of even-A $^{194-210}$Po isotopes, which does not require the introduction of deformed $4p$-$2h$ excitations.

II. PHENOMENOLOGICAL ANALYSIS OF THE POLONIUM SYSTEMATICS

The excitation energy of the 2_1^+ state often provides the simplest gauge of the nuclear shape. The 2_1^+ energies for the Cd and Te isotopes are plotted in Fig. 1(a) as a function of neutron number. These trends can be related qualitatively to the underlying microscopic structure by examining the occupation probabilities of the orbitals in the $N=50$–82 neutron shell. In Fig. 1(b) we display the BCS emptiness parameter (u^2), which was calculated for the neutron states in Sn using a realistic [8] pairing strength $G_n=20/A$ MeV and fixed single-particle energies extracted from ^{131}Sn [9,10]. The initial rapid decrease of the 2_1^+ energies with decreasing neutron number coincides with the opening of the neutron intruder orbital $1h_{11/2}$, which lies near the top of the 50–82 shell. The valence protons in Cd and Te most likely occupy the $1g_{9/2}$ and $1g_{7/2}$ orbitals, respectively. Therefore, the overlap of the wave functions of these high-j, $n_p=n_n$ and $\ell_p\approx\ell_n$ orbitals drives the 2_1^+ states toward a more collective shape.

A similar analysis of the Po systematics reveals a funda-

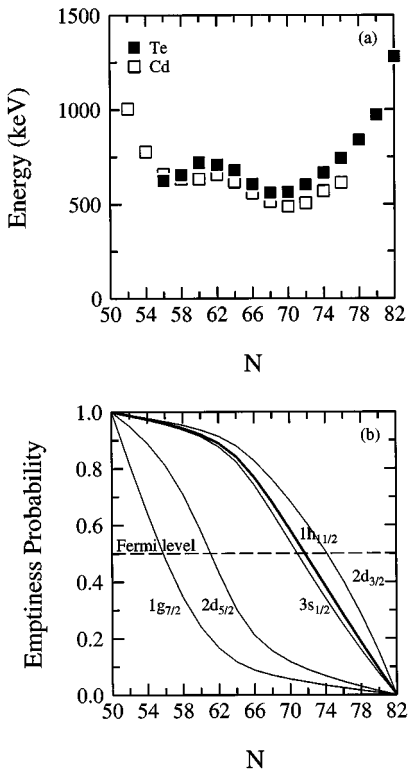

FIG. 1. (a) Energies of the 2_1^+ states in Cd (open symbols) and Te (closed symbols) isotopes [9]. (b) Neutron BCS emptiness parameters u^2 calculated for Sn isotopes with $G_n = 20/A$ MeV. The Fermi level is plotted for reference.

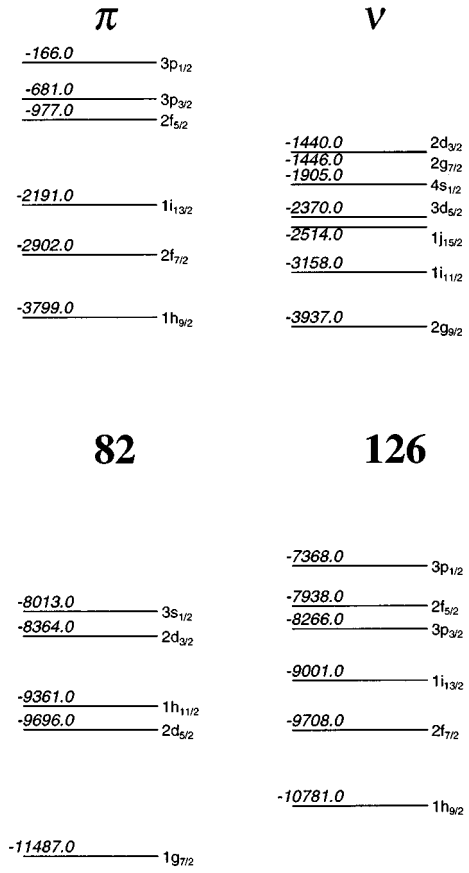

FIG. 2. Single-particle proton and neutron levels, extracted from $^{209}_{83}\mathrm{Bi}_{126}$ and $^{207}_{82}\mathrm{Pb}_{125}$ [10].

mental difference between the 50–82 and 82–126 neutron shells. The single-particle orbitals near ^{208}Pb are displayed in Fig. 2. Because the high-j $1i_{13/2}$ intruder orbital lies deeper in the shell, the overlap argument predicts that the onset of collectivity should be delayed in the Po isotopes. This is indeed borne out by the systematics of the 2_1^+ energies, plotted in Fig. 3(a). Apart from the initial drop in energy from ^{210}Po to ^{208}Po, corresponding to the opening of the neutron shell, the 2_1^+ energies are surprisingly constant down to ^{200}Po. In Fig. 3(b) we display the BCS neutron emptiness calculations with $G_n = 23/A$ MeV and fixed single-particle energies deduced from ^{207}Pb [9,10]. The rapid drop in energies of the 2_1^+ states for $A < 200$ once again occurs when the intruder orbital, $1i_{13/2}$, is near the Fermi surface. When valence neutrons occupy this orbital there should be a good overlap with the wave function for the $1h_{9/2}$ orbital, which is the most likely proton orbital, and the nuclear motion should be more collective.

The systematics of known low-lying states in Po are plotted in Fig. 4. The even-parity states up to the 6_1^+ all show the same rapid increase in collectivity for $A < 200$ as the 2_1^+ states. The energies of the 8_1^+ states continue to increase steadily as the number of neutrons decreases until ^{194}Po. The relative spacings of energy levels within each isotope provide further insight into the evolution of collectivity in this isotopic chain. The trends of the low-lying levels in polonium isotopes smoothly evolve from the textbook [2] shell-model structure of two protons in the $(1h_{9/2})^2$ configuration coupled by a surface delta interaction (SDI) [12], to the evenly spaced levels of an almost perfect harmonic oscillator in ^{196}Po [6], and beyond, to the prerotational [7] structure of ^{194}Po.

The empirical arguments presented here emphasize the importance of the proton $1h_{9/2}$ orbital as well as the role of vibrational degrees of freedom in the polonium isotopes. Furthermore, because the progression is relatively smooth, it is amenable to a description in terms of a single theoretical framework across the systematics. We present such descriptions in terms of the particle-core model (PCM) [13] and the quasiparticle random phase approximation (QRPA) [14]. When the results of these calculations are combined, we obtain a complete picture of the onset of collectivity in the even-*A* polonium isotopes and can understand better the importance of the high-j orbitals.

III. THE PARTICLE-CORE MODEL

A. Theoretical background

Complete derivations of the particle core model (PCM) can be found elsewhere [13,15,16]. We only reproduce the essential results here for easy reference and consistency of notation. In the PCM, a few nucleons (in this case two protons) are coupled to a vibrating core. We assume that the extra-core nucleons move in a vibrating field whose equipotential surfaces adiabatically follow the liquid-drop vibration of the core. Then the dynamical part of the PCM Hamiltonian can be written:

$$\mathbf{H}=\mathbf{H}_{\rm core}+\mathbf{H}_{\rm int}+\mathbf{H}_{\rm res}, \tag{1}$$

where $\mathbf{H}_{\rm core}$ is the harmonic oscillator Hamiltonian for the core, $\mathbf{H}_{\rm int}$ is the interaction Hamiltonian between the core and extra-core nucleons and $\mathbf{H}_{\rm res}$ is the residual interaction between extra-core particles. These various contributions can be written in second quantized form using the phonon creation (annihilation) operators $b^\dagger$ (b):

$$\mathbf{H}_{\rm core}=\hbar\omega_c\left(\sum_{\mu=-2}^{\mu=2} b_\mu^\dagger b_\mu+\frac{5}{2}\right), \tag{2}$$

where $\hbar\omega_c$ is the quadrupole phonon energy of the core. Similarly, the interaction Hamiltonian is written:

$$\mathbf{H}_{\rm int}=-\sqrt{\frac{\pi}{5}}\xi\hbar\omega_c\sum_i\sum_\mu [b_\mu+(-1)^\mu b_\mu^\dagger]Y_{2\mu}(\hat{r}_i), \tag{3}$$

where ξ is the dimensionless particle-core interaction strength and $\hat{r}_i$ is a unit vector in the direction of the ith extra-core particle. The residual interaction $\mathbf{H}_{\rm res}$ is taken to be the surface delta interaction, and can be written in coordinate form as

$$\mathbf{H}_{\rm res}\propto\sum_{i<j}\delta^3(\vec{r}_i-\vec{r}_j)\delta(r_i-R_0) \tag{4}$$

with $R_0\equiv r_0A^{1/3}$. The summation runs over all extra-core particle pairs.

In our PCM calculations, we consider two protons in a fixed $(1h_{9/2})^2$ configuration coupled to a vibrational core of up to $N=4$ quadrupole phonons. The corresponding basis states are written $|N_{\rm ph}J_{\rm ph}\nu_{\rm ph},J;I\rangle$ with $N_{\rm ph},J_{\rm ph},\nu_{\rm ph}$ the phonon number, total angular momentum, and seniority, respectively; J is the angular momentum of the two particles in the $(1h_{9/2})^2$ configuration, and I is the total angular momentum of the particle+core system. The core and residual interaction matrix elements are diagonal in this basis:

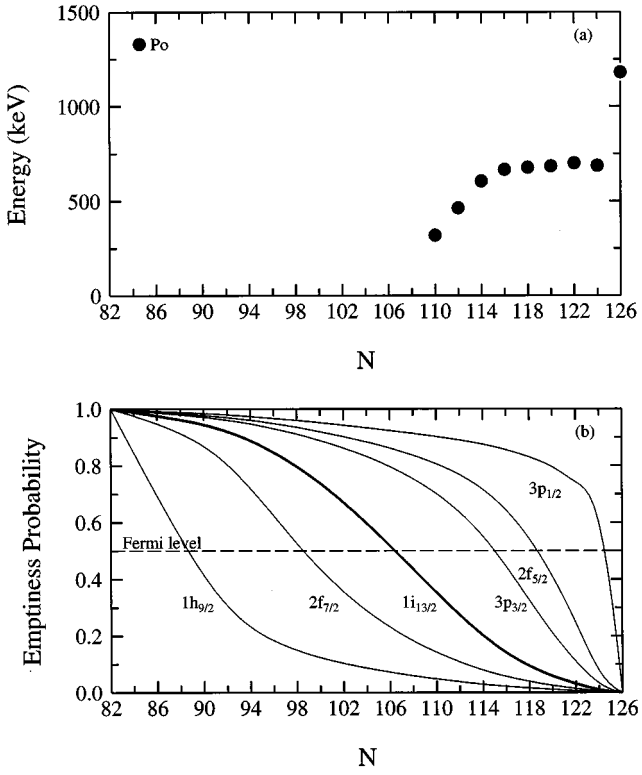

FIG. 3. (a) Energies of the 2_1^+ states in Po isotopes [7,9]. (b) Neutron BCS emptiness parameters u^2 calculated with $G_n=23/A$ MeV. The Fermi level is plotted for reference.

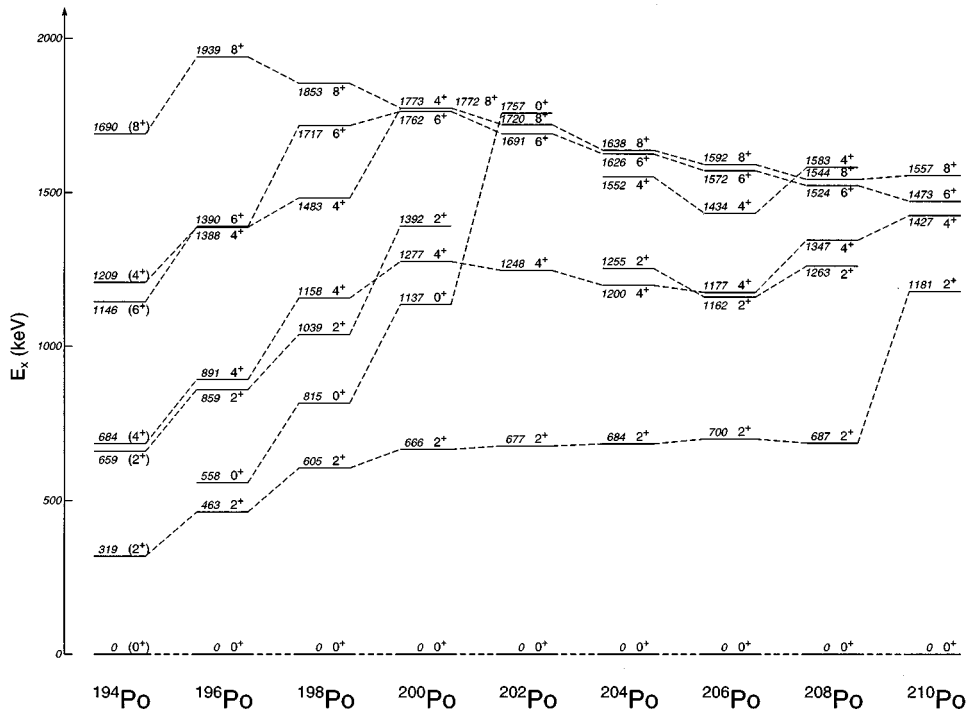

FIG. 4. Energy systematics of low-lying, positive-parity states in even-A Po isotopes. Data taken from [6,7,9,11].

$$\langle N'_{\rm ph}J'_{\rm ph}\nu'_{\rm ph},J';I|\mathbf{H}_{\rm core}|N_{\rm ph}J_{\rm ph}\nu_{\rm ph},J;I\rangle=\hbar\omega_c\left(N+\frac{5}{2}\right)\delta_{N'_{\rm ph}N_{\rm ph}}\delta_{J'_{\rm ph}J_{\rm ph}}\delta_{\nu'_{\rm ph}\nu_{\rm ph}}\delta_{J'J}, \tag{5}$$

$$\langle N'_{\rm ph}J'_{\rm ph}\nu'_{\rm ph},J';I|\mathbf{H}_{\rm res}|N_{\rm ph}J_{\rm ph}\nu_{\rm ph},J;I\rangle=-G\hbar\omega_c\frac{16}{3}\frac{j(j+1)}{2j+1}\begin{pmatrix} j & j & J\\ 1/2 & -1/2 & 0\end{pmatrix}^2\delta_{N'_{\rm ph}N_{\rm ph}}\delta_{J'_{\rm ph}J_{\rm ph}}\delta_{\nu'_{\rm ph}\nu_{\rm ph}}\delta_{J'J} \tag{6}$$

with $j=9/2$ in our case. The dimensionless SDI strength G is chosen such that $G\hbar\omega_c$ is the difference between matrix elements with $J=0$ and $J=2$ in Eq. (6). The interaction matrix elements can also be calculated:

$$\begin{aligned}\langle N'_{\rm ph}J'_{\rm ph}\nu'_{\rm ph},J';I|\mathbf{H}_{\rm int}|N_{\rm ph}J_{\rm ph}\nu_{\rm ph},J;I\rangle=&-\xi\hbar\omega_c(2j+1)\sqrt{(2J+1)(2J'+1)}(-1)^{I+j+1/2}\begin{Bmatrix} I & J' & J'_{\rm ph}\\ 2 & J_{\rm ph} & J\end{Bmatrix}\begin{Bmatrix} j & j & 2\\ J & J' & j\end{Bmatrix}\\ &\times\begin{pmatrix} j & 2 & j\\ -1/2 & 0 & 1/2\end{pmatrix}[(-1)^{J_{\rm ph}}\langle N'_{\rm ph}J'_{\rm ph}\nu'_{\rm ph}\|b^\dagger\|N_{\rm ph}J_{\rm ph}\nu_{\rm ph}\rangle\\ &+(-1)^{J'_{\rm ph}}\langle N_{\rm ph}J_{\rm ph}\nu_{\rm ph}\|b^\dagger\|N'_{\rm ph}J'_{\rm ph}\nu'_{\rm ph}\rangle].\end{aligned} \tag{7}$$

The reduced matrix elements $\langle\cdots\|b^\dagger\|\cdots\rangle$ of the phonon operators are tabulated in [15–17]. For each particular choice of the model parameters, $\hbar\omega_c$, $G\hbar\omega_c$, and $\xi\hbar\omega_c$, the PCM Hamiltonian in Eq. (1) can be diagonalized numerically.[1]

B. Application of the PCM to the polonium isotopes

In the heavier polonium isotopes, the two protons beyond the closed $Z=82$ shell likely occupy the $1h_{9/2}$ orbital. This assertion is supported by single-particle proton levels deduced [10] from states in ^{209}Bi [9]. The unperturbed size of the $Z=82$ shell gap is $\approx$ 4 MeV, while the next orbital beyond the $1h_{9/2}$, the $2f_{7/2}$ orbital, lies $\approx$ 1 MeV higher. As the number of valence neutrons is increased, these gaps can be reduced by the residual p-n interaction. In the PCM calculations, we assume that the $(1h_{9/2})^2$ configuration dominates the proton contribution. This assumption will be tested by the success of the model in fitting the Po systematics and by the QRPA calculations discussed below, which include a residual quadrupole p-n interaction.

In order to fit the $^{194-208}$Po energy systematics consistently, the parameters are given explicit dependencies on the mass number A. The SDI strength $G\hbar\omega_c$ is expected [15] to follow a $1/A$ dependence. Likewise, the phonon energy $\hbar\omega_c$ is predicted [18] by hydrodynamic principles to follow a slow $\sqrt{1/A-\text{const}/A^2}$ dependence, although substantial deviations from this estimate are found throughout the nuclear chart. In a first calculation (fit I), $\hbar\omega_c$ is assumed to be constant across the systematics, to reduce the number of free parameters in the model. By contrast, there are no simple estimates of the particle-core coupling strength $\xi\hbar\omega_c$. The phenomenological analysis discussed above suggests that this parameter should depend on the microscopic structure of the neutron configuration, which does not follow a simple mass dependence. In light of that analysis, $\xi\hbar\omega_c$ is kept constant for $A=200-208$ and allowed to vary freely in each isotope with $A<200$. Thus, there are altogether six free parameters in this implementation of the PCM.

Positive-parity levels to be included in the fit are chosen according to two criteria: (1) they must be known experimentally for most nuclei to be fit and (2) only states with $I\leqslant 8$ are included because of the truncation of the proton basis to the $(1h_{9/2})^2$ configuration and phonon basis to $N_{\rm ph}\leqslant 4$. With these restrictions, the 2_1^+, 2_2^+, 4_1^+, 4_2^+, 6_1^+, and 8_1^+ states in 9 isotopes are included in the fit, yielding 46 levels altogether.

The energy levels were fit by iterative χ^2 minimization. The experimental uncertainties in measured excitation energies could not be used in the χ^2 method, because inherent limitations in the model preclude a fit within measured precision. Instead, a fixed uncertainty σ_E was used for each level energy. The χ^2 then scales as $1/\sigma_E^2$ and the uncertainties on individual parameters scale as σ_E. The best fit (fit I) yields $\chi^2/\nu=7.57\times10^{-3}/\sigma_E^2$, and the corresponding parameters are given in Table I. The fits to yrast and non-yrast energy levels are plotted in Figs. 5(a) and 5b, respectively. In general, the fit is quite good, especially for $A<200$. The most serious deviation occurs for the 8_1^+ states, whose energies are not reproduced below $A=200$. This isolated failure of the model might be attributable to the truncations of the configuration spaces for both the proton and phonon components. It is a remarkable result that, since the phonon energy is held constant and the residual proton interaction strength

TABLE I. PCM parameters for fit I described in text. To show the quality of the χ^2 minimum, we have assumed an overall energy uncertainty σ_E = 0.050 MeV. In this case, $\chi^2/\nu=3.0$.

Parameter	Value (MeV)
$\hbar\omega_c$	0.623 ± 0.035
$G\hbar\omega_c\times A$	274.4 ± 12.4
$\xi\hbar\omega_c(A=194)$	2.356 ± 0.701
$\xi\hbar\omega_c(A=196)$	1.638 ± 0.520
$\xi\hbar\omega_c(A=198)$	0.819 ± 0.595
$\xi\hbar\omega_c(A\geqslant200)$	0.000 ± 0.954

[1]We have written a code to diagonalize the PCM Hamiltonian and applied it to the Po isotopes.

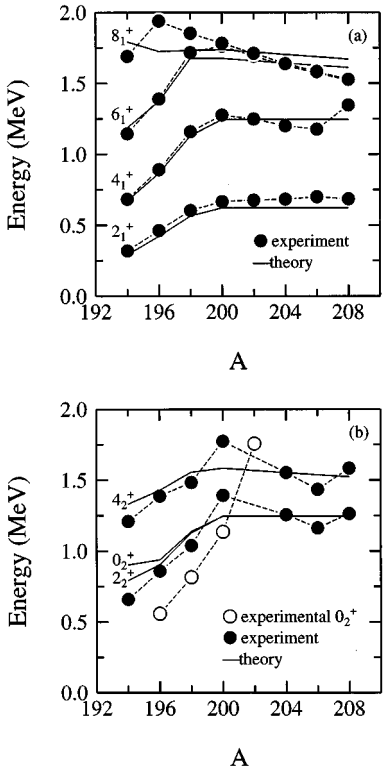

FIG. 5. Best fit from the PCM calculations in $^{194-208}$Po of (a) the yrast energy levels and (b) the nonyrast levels. The solid symbols connected by dotted lines are the experimental values. The solid lines are the PCM results. In (b) the open symbols are the 0_2^+ states, which were not used to determine the parameters. Data are taken from [6,7,9,11].

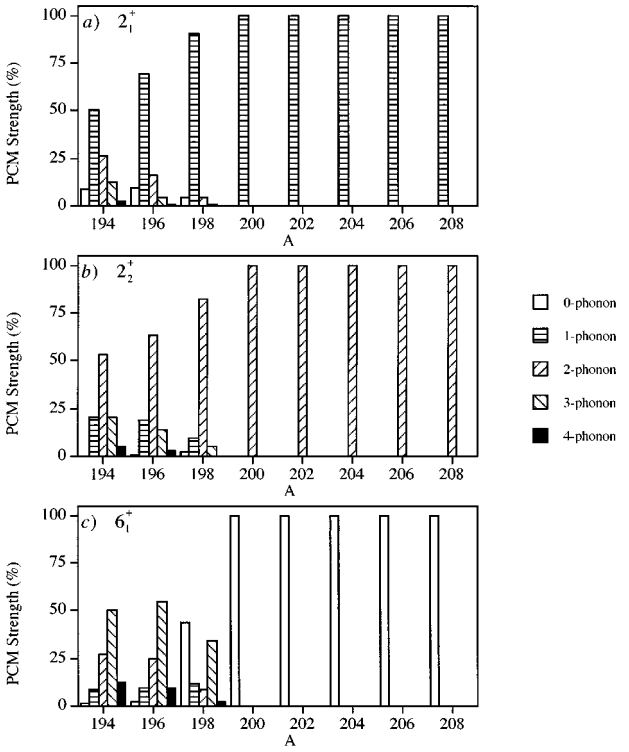

FIG. 6. Plot of the PCM strength coefficients $c_I^2(N_{\rm ph})$ defined in Eq. (9) for (a) the 2_1^+ states, (b) the 2_2^+ states, and (c) the 6_1^+ states in the Po isotopes.

varies slowly, the remaining trends for $A<200$ are accurately reproduced by a sharp rise of the proton-core interaction parameter alone. The robustness of this conclusion was tested [16] by allowing both $\hbar\omega_c$ and $\xi\hbar\omega_c$ to vary freely in each $^{194-208}$Po isotope (fit II). It was found that, apart from a sudden increase at ^{200}Po, the phonon energy remains fairly constant with an average value of 0.624(21) MeV. The proton-core strength $\xi\hbar\omega_c$ was also much larger in ^{200}Po than in the present calculations; the fit to the non-yrast 2_2^+ and 4_2^+ states was improved, but the smooth trends in the global parameters were lost. There was no visible improvement in fit II to the 8_1^+ states below $A=200$.

The PCM wave functions can also be calculated for fit I to illustrate the evolution of collectivity in Po isotopes as a function of neutron number and angular momentum. In general, the eigenfunctions of the PCM Hamiltonian can be written

$$|\psi\rangle=\sum_\alpha c_\alpha|N_{\rm ph}^\alpha J_{\rm ph}^\alpha \nu_{\rm ph}^\alpha, J^\alpha; I\rangle. \tag{8}$$

The number of significant terms in these wave functions can be large, especially when state mixing and collectivity occur. A more compact representation of the wave functions is obtained by plotting the sum of the coefficients for a given number of phonons in the wave function:

$$c_I^2(N_{\rm ph})\equiv\sum_{J_{\rm ph}^\alpha \nu_{\rm ph}^\alpha, J^\alpha} c_\alpha^2. \tag{9}$$

This emphasizes the phonon degrees of freedom. These coefficients are plotted for the 2_1^+, 2_2^+, and 6_1^+ states in Fig. 6. All of these calculated phonon wave functions display the same general behavior: they are remarkably pure for $A\geqslant 200$ and become rapidly and increasingly mixed for $A<200$. The 2_1^+ and 2_2^+ levels, shown in Fig. 6, are collective one- and two-phonon states, respectively, in $^{200-208}$Po. The gradual mixing observed in $A<200$ isotopes signals a change in the intrinsic structure of the phonon core. For the 6_1^+ state, the change from a pure zero-phonon [i.e., $(\pi 1h_{9/2})^2$] to a very mixed phonon configuration is more sudden, but also marks a change in the structure from ^{200}Po to ^{198}Po.

We have not attempted to predict $B(E2)$ values between states in the PCM. To calculate transitions would require effective charges for both the phonon and two-particle components, free parameters which cannot be fixed by the very limited transition probability data available. Instead, because it provides a more complete semimicroscopic description, the QRPA was used to estimate $B(E2)$ values for the Po nuclei.

The success of the PCM with a constant core phonon energy and rapidly increasing proton-core strength for $A<200$ Po isotopes could mean either that the microscopic character of the phenomenological phonons changes for $A<200$ or that the interaction itself changes. However, the rise of the particle-core coupling strength for $A<200$ Po iso-

topes occurs exactly when the occupation probability, u^2, for the $\nu 1i_{13/2}$ orbital increases as displayed in Fig. 3. This suggests a microscopic interpretation in which specific orbitals occupied by the neutrons drive the onset of collective motion in Po isotopes. These arguments, however, do not provide a clear and complete picture of the microscopic evolution of collectivity in polonium. The PCM assumes phenomenological phonons with no explicit microscopic structure, and the simple pairing picture ignores the *p*-*n* interaction altogether. In short, what is required is a model which treats both protons and neutrons on an equal footing and can build collective excitations from interacting configurations of both types of nucleons. The quasiparticle random phase approximation (QRPA) implements this approach in a mathematically tractable form.

IV. THE QUASIPARTICLE RANDOM PHASE APPROXIMATION

A. Theoretical background

Detailed derivations of the QRPA can be found elsewhere [8,14,16], and again, only the essential results are summarized here. In this approximation, a realistic residual nucleon-nucleon interaction can be diagonalized in a large single-particle configuration basis. In this paper we use a short-range pairing interaction between like particles and a long-range quadrupole *p*-*n* interaction, using the proton and neutron single-particle states displayed in Fig. 2. The *p*-*p* and *n*-*n* interactions are diagonalized first, using standard BCS theory [8]. Excitations in even-even nuclei can then be decomposed into excitations of quasiproton or quasineutron pairs given by the tensor product:

$$A^{\dagger}_{(j_1 j_2)^J_M} \equiv [\alpha^{\dagger}_{j_1 m_1} \otimes \alpha^{\dagger}_{j_2 m_2}]^J_M = \sum_{m_1 m_2} \langle j_1 m_1 j_2 m_2 | JM \rangle \alpha^{\dagger}_{j_1 m_1} \alpha^{\dagger}_{j_2 m_2}, \quad (10)$$

where $\alpha^{\dagger}_{jm}$ creates a quasiparticle state (jm). Each quasiparticle pair is created with energy:

$$E(j_1,j_2) = \sqrt{(\epsilon_{j_1}-\lambda)^2+\Delta^2} + \sqrt{(\epsilon_{j_2}-\lambda)^2+\Delta^2}, \quad (11)$$

where the ϵ_j are single-particle energies, λ is the Fermi surface energy, and Δ the gap parameter. Collective phonon excitations in the QRPA can then be expanded in this quasiparticle pair basis. The corresponding quadrupole phonon excitation operator is a tensor with components

$$\Theta^{\dagger}_{\mu} \equiv \frac{1}{2}\sum_{jj'} [\psi_{jj'} A^{\dagger}_{(jj')^{J=2}_{\mu}} - (-1)^{\mu} \phi_{jj'} A_{(jj')^{J=2}_{-\mu}}]. \quad (12)$$

For a quasiproton (quasineutron) pair excitation the indices jj' run over all proton (neutron) states in the configuration space. The coefficients $\psi_{jj'}$ and $\phi_{jj'}$ give the amplitude for the creation and annihilation, respectively, of the coupled quasiparticle pair $(jj')^{J=2}$.

The residual, quadrupole *p*-*n* interaction can also be written in a quasiparticle basis, and diagonalized in the random phase approximation (RPA). For a quadrupole interaction $\mathbf{Q}\cdot\mathbf{Q}$ of given strength χ_{pn}, this procedure yields a dispersion equation which can be solved numerically[2] for the 2^+ eigenvalues, $\hbar\omega$:

$$1 - \chi^2_{pn} S_p S_n = 0, \quad (13)$$

where we have defined the sums

$$S_p \equiv 2\sum_{j_p j'_p} \frac{[F(j_p,j'_p)]^2 E(j_p,j'_p) u^2_{j_p j'_p}}{[E(j_p,j'_p)]^2 - (\hbar\omega)^2},$$

$$S_n \equiv 2\sum_{j_n j'_n} \frac{[F(j_n,j'_n)]^2 E(j_n,j'_n) u^2_{j_n j'_n}}{[E(j_n,j'_n)]^2 - (\hbar\omega)^2}. \quad (14)$$

The reduced quadrupole moments,

$$F(j_1,j_2) \equiv \frac{1}{\sqrt{5}} \langle N_2 \ell_2 j_2 \| -M\omega_0 r^2 \mathbf{Y}_2 \| N_1 \ell_1 j_1 \rangle, \quad (15)$$

are defined in terms of harmonic oscillator wave functions and are tabulated in [8]. In the case of an attractive *p*-*n* interaction (i.e., $\chi_{pn}>0$), one eigenvalue $\hbar\omega$, corresponding to the collective eigenstate, will be lowered with respect to the others. To each eigenvalue $\hbar\omega$ corresponds an eigenvector with proton and neutron components:

$$\psi^p_{j_p j'_p} = \mathcal{N} \frac{\sqrt{S_n} F(j_p,j'_p) u_{j_p j'_p}}{E(j_p,j'_p) - \hbar\omega},$$

$$\phi^p_{j_p j'_p} = \mathcal{N} \frac{\sqrt{S_n} F(j_p,j'_p) u_{j_p j'_p}}{E(j_p,j'_p) + \hbar\omega},$$

$$\psi^n_{j_n j'_n} = \mathcal{N} \frac{\sqrt{S_p} F(j_n,j'_n) u_{j_n j'_n}}{E(j_n,j'_n) - \hbar\omega},$$

$$\phi^n_{j_n j'_n} = \mathcal{N} \frac{\sqrt{S_p} F(j_n,j'_n) u_{j_n j'_n}}{E(j_n,j'_n) + \hbar\omega}, \quad (16)$$

where we have defined $u_{jj'} \equiv u_j v_{j'} + u_{j'} v_j$, and the overall normalization constant $\mathcal{N}$ is determined from

$$\frac{1}{2}\sum_{j_p,j'_p} [(\psi^p_{j_p j'_p})^2 - (\phi^p_{j_p j'_p})^2] + \frac{1}{2}\sum_{j_n,j'_n} [(\psi^n_{j_n j'_n})^2 - (\phi^n_{j_n j'_n})^2] = 1. \quad (17)$$

The reduced $E2$ transition strength from the one-phonon state is given by [8]

[2]We have written a code to calculate the eigenvalues and eigenfunctions of the QRPA with a quadrupole *p*-*n* interaction, and applied it to the Po isotopes.

$$B(E2;2_1^+\rightarrow 0_1^+)=\frac{e^2}{2}\Bigg[(1+\delta e_p)\sum_{j_pj_p'}F^2(j_p,j_p')g_{j_pj_p'}u_{j_pj_p'}+\delta e_n\sum_{j_nj_n'}F^2(j_n,j_n')g_{j_nj_n'}u_{j_nj_n'}\Bigg]^2, \quad (18)$$

where

$$g_{jj'}=\sqrt{\frac{2}{\mathcal{G}}}\times\frac{F(j,j')u_{jj'}E(j,j')}{E^2(j,j')-(\hbar\omega)^2} \quad (19)$$

and

$$\mathcal{G}=\frac{F^2(j,j')u_{jj'}^2\hbar\omega E(j,j')}{[E^2(j,j')-(\hbar\omega)^2]^2}. \quad (20)$$

The effective charge increments, δe_p and δe_n, for the proton and neutron, respectively, are free parameters.

B. Application of the QRPA to the polonium isotopes

The PCM calculations have already provided a successful description of the energy systematics of even-A $^{194-208}$Po isotopes. The wave functions of all states fit in the model were seen to maintain a predominantly pure, single-phonon configuration for $A\geqslant 200$ and become fragmented for $A<200$, which was interpreted as a signature of the onset of collectivity in those states. The QRPA calculations presented here are not intended to provide a second parametric fit to the data. Rather, they will be used to extract a semimicroscopic wave function for the 2_1^+ states, and thereby provide a clearer microscopic understanding of the phenomenological phonons in the PCM framework.

The pairing strengths G_p and G_n for polonium were extracted first, by fitting BCS predictions [8] of pairing energies to their experimental values. The proton and neutron pairing energies $P_p(Z,N)$ and $P_n(Z,N)$ are defined as

$$P_p(Z,N)\equiv\frac{1}{2}[2BE(Z-1,N)-BE(Z,N)-BE(Z-2,N)],$$

$$P_n(Z,N)\equiv\frac{1}{2}[2BE(Z,N-1)-BE(Z,N)-BE(Z,N-2)], \quad (21)$$

and the experimental binding energies $BE(Z,N)$ are taken from [19]. The single-particle basis states are those displayed in Fig. 2. The best fit was found [16] for $G_p=24.3^{+0.2}_{-0.2}/A$ MeV and $G_n=19.7^{+0.2}_{-0.1}/A$ MeV. Next, the proton-neutron strength χ_{pn} was extracted in each isotope by solving the QRPA dispersion equation, Eq. (13), with $\hbar\omega\equiv E_x(2_1^+)$. Then, the wave function components in Eq. (16) could be evaluated for each nucleus. The proton and neutron component strengths, defined as

$$\mathcal{C}^p_{j_pj_p'}\equiv\frac{1}{2}[(\psi^p_{j_pj_p'})^2-(\phi^p_{j_pj_p'})^2],$$

$$\mathcal{C}^n_{j_nj_n'}\equiv\frac{1}{2}[(\psi^n_{j_nj_n'})^2-(\phi^n_{j_nj_n'})^2], \quad (22)$$

TABLE II. QRPA predictions for $^{194-208}$Po $B(E2;2_1^+\rightarrow 0_1^+)$ values in single-particle units (spu) calculated with effective charges $\delta e_p = \delta e_n = 0.39$.

A	$B(E2;2_1^+\rightarrow 0_1^+)$ (spu)
194	16.4
196	9.8
198	6.5
200	4.8
202	3.7
204	2.9
206	2.3
208	1.7

are plotted for the first few leading strengths in Figs. 7(a) and 7(b), respectively.

The proton wave function is clearly dominated by the $(1h_{9/2})^2$ quasiparticle pair configuration, with weak contributions from excitations across the shell gap involving the $1h_{11/2}$ orbital. The neutron wave function consists of a mixture of low-j quasineutron pairs for $A>200$, with a rising contribution from the quasiparticle pair $(1i_{13/2})^2$, which becomes dominant for $A<200$. The reduced transition strengths were calculated using the effective charge increments $\delta e_p = \delta e_n = 0.39$, which correctly reproduce the known [9] $B(E2;2_1^+\rightarrow 0_1^+)$ value in ^{210}Po. The $B(E2;2_1^+\rightarrow 0_1^+)$ values listed in Table II are consistent with weakly collective motion.

The value of the quadrupole-quadrupole interaction strength, χ_{pn}, extracted from Eq. (13) was found to be es-

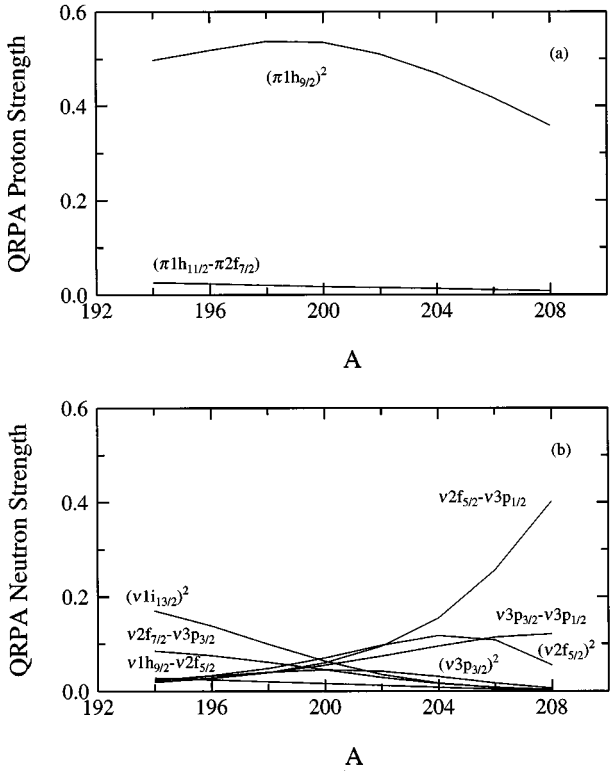

FIG. 7. Plot of the first few leading QRPA component strengths defined in Eq. (22) for (a) the protons and (b) the neutrons, in the Po isotopes.

sentially constant across the $^{194-208}$Po systematics. The constancy of this parameter further suggests that it is the specific active orbitals involved, rather than an increased proton-neutron strength, which are directly responsible for the behavior of the 2_1^+ states. Direct comparison between the PCM and QRPA wave functions of the 2_1^+ states shows that the pure one-phonon configurations which hold for $A>200$ in the PCM correspond to a mixture of low-j quasineutron pairs in the QRPA. Conversely, the fragmentation of the PCM wave functions parallels the rise of the quasineutron $(1i_{13/2})^2$ contribution to the 2_1^+ state wave functions.

V. CONCLUSION

We have presented a consistent picture of the onset of collectivity in polonium isotopes using complementary descriptions in the particle-core model and the quasiparticle random phase approximation. In the polonium systematics, the first important change in structure occurs between the semimagic ^{210}Po and ^{208}Po, as evidenced by the drop in 2_1^+ energies from 1.181 to 0.687 MeV. The 2_1^+ energies then remain remarkably constant, until ^{200}Po, where a second, more gradual decrease begins. The PCM provides a very good fit to low-lying, positive-parity states in $^{194-208}$Po. The observed change in structure for $A<200$ is accurately reproduced by a rapid increase in the particle-core interaction strength. This model successfully reproduces trends across isotopes, as well as energy spacings within each nucleus. However, its fundamental assumption of a macroscopic, liquid-drop, vibrating core precludes any insight into the microscopic nature of the vibration. To circumvent this limitation, the QRPA was used to extract semimicroscopic wave functions for the 2_1^+ states, which should be the analogs of the phonons in the PCM calculations. The QRPA predicts a relatively constant quasiproton $(1h_{9/2})^2$ configuration, with weak contributions from excitations across the shell gap. Conversely, the quasineutron configuration changes from a mixture of low-j pairs for $A>200$, where the PCM wave function consists of a pure one-phonon component, to a configuration increasingly dominated by the $(1i_{13/2})^2$ quasineutron pair. Although the phonon energy remains constant throughout the systematics in the PCM, the QRPA reveals a dramatic change in the microscopic structure of the collective excitations. Indeed, the drive toward the almost ideal vibrational structure of ^{196}Po [6] and the increased collectivity in ^{194}Po [7] occurs only when the $\nu 1i_{13/2}$ orbital becomes the dominant component in the wave function.

These results emphasize the critical role of the $\pi 1h_{9/2}$ and $\nu 1i_{13/2}$ orbitals in the onset of collectivity in polonium. Remarkably however, the PCM and QRPA can account for the fitted systematics with little or no need for the added collectivity of particle-hole intruder structures. This conclusion is also supported [6] by the paucity of evidence for strongly collective bands or the enhanced selection rules expected between states with $4p$-$2h$ mixtures.

Nevertheless, the limitations of both the PCM and QRPA must be recognized, and the ensuing conclusions weighed accordingly. The particle-core model, in particular, fails to reproduce the 0_2^+ state systematics, which have now been measured [11] in $^{196-202}$Po. For $A\leqslant 200$, the experimental 0_2^+ state appears more collective than the PCM predictions, and particle-hole intruder excitations may well play an important role for this level. However, there is no compelling evidence for excitations built upon this proposed $4p$-$2h$ configuration; the nonyrast 2_2^+ and 4_2^+ states can be satisfactorily described as predominantly multi-phonon excitations. The QRPA calculations also carry inherent limitations. For example, the residual interaction was simplified by assuming the quadrupole interaction acts between unlike particles only. Traditionally [8,14], pairing+quadrupole QRPA calculations have included a residual quadrupole interaction between protons (with strength χ_p) and neutrons (with strength χ_n) as well. Our assumption, which is equivalent to setting $\chi_p=\chi_n=0$, reduces the number of parameters, while emphasizing the role of the p-n interaction in driving the collective motion. Finally, for simplicity, the model was truncated to two-quasiparticle excitations. If intruder configurations were to play a significant role, four-quasiparticle excitations would have to be included as well.

The question of the nature of the mechanisms which drive the collectivity in polonium isotopes is best answered by experimental observables. Unfortunately, the experimental quantities which would provide the most stringent restrictions on theoretical models, e.g., absolute $B(E2)$ values, g-factors, $E0$ transitions strengths, etc., are difficult, if not impossible, to measure in neutron-deficient polonium isotopes. The difficulties are twofold. First these nuclei can only be formed in heavy-ion reactions with low fusion cross sections which are dominated by fission. Second, there are a plethora of isomers in these nuclei [9], including the long-lived (several hundred ns) yrast 11^- isomers, through which a large fraction of the population of low-lying states proceeds. Such isomers preclude the measurements of lifetimes by traditional Doppler techniques. Given these restrictions, fits to energy systematics remain the dominant probe of the onset of collective motion in polonium isotopes.

ACKNOWLEDGMENTS

We would like to thank Professor R. F. Casten and Professor L. Zamick for stimulating discussions. This work was supported in part by the National Science Foundation.

[1] A. De-Shalit and M. Goldhaber, Phys. Rev. **92**, 1211 (1953).

[2] R.F. Casten, *Nuclear Structure from a Simple Perspective* (Oxford University Press, New York, 1990).

[3] J.L. Wood, K. Heyde, W. Nazarewicz, M. Huyse, and P. van Duppen, Phys. Rep. **215**, 101 (1992).

[4] C.S. Lee *et al.*, Nucl. Phys. **A528**, 381 (1991); **A530**, 58 (1991).

[5] J.A. Cizewski, L. A. Bernstein, R.G. Henry, H.-Q. Jin, C.S. Lee, and W. Younes, in *Capture Gamma-Ray Spectroscopy*, edited by J. Kern (World Scientific, Singapore, 1994), p. 328.

[6] L.A. Bernstein *et al.*, Phys. Rev. C **52**, 621 (1995).
[7] W. Younes *et al.*, Phys. Rev. C **52**, R1723 (1995).
[8] V.G. Soloviev, *Theory of Complex Nuclei* (Pergamon, New York, 1976).
[9] Evaluated Nuclear Structure Data Files, Brookhaven National Laboratory, Upton, NY.
[10] T.T.S. Kuo and G.H. Herling, U.S. Naval Research Laboratory Report No. 2258, 1971 (unpublished).
[11] N. Bijnens *et al.*, Phys. Rev. Lett. **75**, 4571 (1995).
[12] A. Plastino, R. Arvieu, and S.A. Moszkowski, Phys. Rev. **145**, 837 (1966).
[13] K. Heyde and P.J. Brussaard, Nucl. Phys. **A104**, 81 (1967).
[14] L.S. Kisslinger and R.A. Sorensen, Rev. Mod. Phys. **35**, 853 (1963).
[15] P.J. Brussaard and P.W.M. Glaudemans, *Shell-Model Applications in Nuclear Spectroscopy* (North-Holland, Amsterdam, 1977).
[16] W. Younes, Ph.D. thesis, Rutgers University, 1996 (unpublished).
[17] B.J. Raz, Phys. Rev. **114**, 1116 (1959).
[18] G. Alaga, in *Proceedings of the International School of Physics ''Enrico Fermi,''* Course XV (Academic Press, New York, 1969), p. 28.
[19] G. Audi and A.H. Wapstra, Nucl. Phys. **A565**, 1 (1993).